Mathematical Biosciences and Engineering

MBE, 21(6): 1–12.
DOI: 10.3934/mbe.2024277
Received: 04 January 2024
Revised: 30 April 2024
Accepted: 11 June 2024
Published: 19 June 2024

http://www.aimspress.com/journal/MBE

Research article

Optimal vaccine allocation strategy: Theory and application to the early stage of COVID-19 in Japan

Toshikazu Kuniya[1,*], Taisuke Nakata[2] and Daisuke Fujii[3]

[1] Graduate School of System Informatics, Kobe University, 1-1 Rokkodai-cho, Nada-ku, Kobe 657-8501, Japan
[2] Graduate School of Economics and Graduate School of Public Policy, University of Tokyo, 7-3-1, Hongo, Bunkyo-ku, Tokyo 113-0033, Japan
[3] Research Institute of Economy, Trade and Industry, 1-3-1, Kasumigaseki Chiyoda-ku, Tokyo 100-8901, Japan

* **Correspondence:** Email: tkuniya@port.kobe-u.ac.jp; Tel: +788036224.

Supplementary

Mathematical model

The main model in this study is the following PDEs system (see Figure S1)[1]:

$$\partial_t S = -\lambda(t,a)S - v(t,a)S,$$
$$\partial_t E = \lambda(t,a)S - \varepsilon E - v(t,a)E,$$
$$\partial_t I = \varepsilon E - \gamma I - v(t,a)I,$$
$$\partial_t R = [1-d(a)]\gamma I - v(t,a)R,$$
$$\partial_t W = d(a)\gamma I - \omega W,$$
$$\partial_t S_h = -\lambda(t,a)S_h,$$
$$\partial_t E_h = \lambda(t,a)S_h - \varepsilon E_h,$$
$$\partial_t I_h = \varepsilon E_h - \gamma I_h,$$
$$\partial_t R_h = [1-d(a)]\gamma I_h,$$

[1] We disregard the aging process assuming $\partial_a S = 0$, $\partial_a E = 0$, …, etc., because the time span of our simulation is less than 1 year.

$$\partial_t W_h = d(a)\gamma I_h - \omega W_h,$$
$$(\partial_t + \partial_\tau)S_v = -[1-\sigma(\tau)]\lambda(t,a)S_v,$$
$$(\partial_t + \partial_\tau)E_v = [1-\sigma(\tau)]\lambda(t,a)S_v - \varepsilon E_v,$$
$$(\partial_t + \partial_\tau)I_v = \varepsilon E_v - \gamma I_v,$$
$$(\partial_t + \partial_\tau)R_v = \{1-[1-\delta(\tau)]d(a)\}\gamma I_v,$$
$$\partial_t W_v = \int_0^{\tau_{max}} [1-\delta(\tau)]d(a)\gamma I_v d\tau - \omega W_v,$$
$$S_v(t,a,0) = v(t,a)S(t,a),\ E_v(t,a,0) = v(t,a)E(t,a),$$
$$I_v(t,a,0) = v(t,a)I(t,a),\ R_v(t,a,0) = v(t,a)R(t,a),$$
$$S(0,a) = [1-h(a)]S_0(a),\ E(0,a) = [1-h(a)]E_0(a),$$
$$I(0,a) = [1-h(a)]I_0(a),\ R(0,a) = [1-h(a)]R_0(a),\ W(0,a) = [1-h(a)]W_0(a),$$
$$S_h(0,a) = h(a)S_0(a),\ E_h(0,a) = h(a)E_0(a),\ I_h(0,a) = h(a)I_0(a),\ R_h(0,a) = h(a)R_0(a),$$
$$W_h(0,a) = h(a)W_0(a),\ S_v(0,a,0) = E_v(0,a,0) = I_v(0,a,0) = R_v(0,a,0) = W_v(0,a) = 0,$$
$$\lambda(t,a) = \int_0^{a_{max}} \beta(a,b)\left[I(t,b) + I_h(t,b) + \int_0^{\tau_{max}} I_v(t,b,\tau)d\tau\right]db.$$

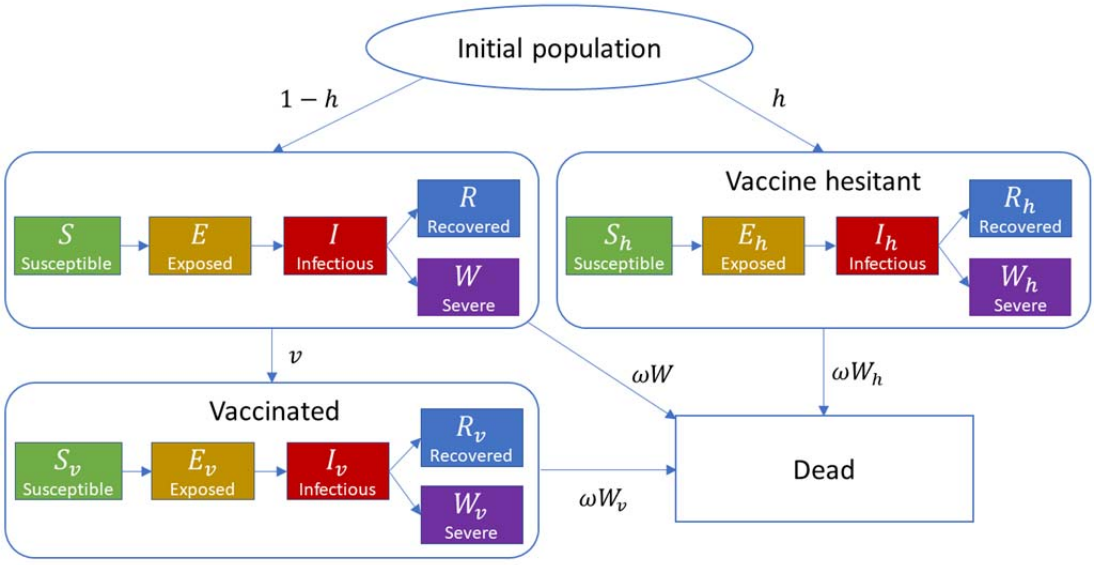

Figure S1. Transfer diagram of our model.

The description of each symbol is as follows (see also Table S1):

- t $(0 \le t \le t_{max})$: time;
- a $(0 \le a \le a_{max})$: age;
- τ $(0 \le \tau \le \tau_{max})$: vaccine age (time elapsed since the first vaccination);
- $S = S(t,a)$: susceptible population;
- $S_h = S_h(t,a)$: vaccinated susceptible population;
- $S_v = S_v(t,a,\tau)$: susceptible population who have been vaccinated;
- $E = E(t,a)$: exposed (pre-infectious) population;
- $E_h = E_h(t,a)$: exposed population with vaccine hesitancy;
- $E_v = E_v(t,a,\tau)$: vaccinated exposed population;
- $I = I(t,a)$: infectious (with and without symptoms) population;

- $I_h = I_h(t,a)$: infectious population with vaccine hesitancy;
- $I_v = I_v(t,a,\tau)$: vaccinated infectious population;
- $R = R(t,a)$: recovered population;
- $R_h = R_h(t,a)$: recovered population with vaccine hesitancy;
- $R_v = R_v(t,a,\tau)$: vaccinated recovered population;
- $W = W(t,a)$: severe population;
- $W_h = W_h(t,a)$: severe population with vaccine hesitancy;
- $W_v = W_v(t,a)$: vaccinated severe population;
- $\lambda(t,a)$: force of infection;
- $v(t,a)$: vaccination rate;
- ε: transition rate from the exposed class to the infectious class;
- γ: removal rate;
- $d(a)$: ratio at which an infected individual enters the severe class;
- ω: mortality rate of severe individuals;
- $\sigma(\tau)$: vaccine efficacy to reduce the infection risk;
- $\delta(\tau)$: vaccine efficacy to reduce the mortality risk;
- $h(a)$: vaccine hesitancy rate;
- $\beta(a,b)$: transmission function between susceptible individuals of age a and infectious individuals of age b.

Table S1. The parameter values in our model.

Symbol	Meaning	Value	Unit	Reference
t	Time	0 – 232	day	-
a	Age	0 – 100	year	-
τ	Vaccine age	0 – 232	day	-
$v(t,a)$	Vaccination rate	(1)	day^{-1}	[5]
ε	Transition rate from exposed to infectious	0.2	day^{-1}	[1,2]
γ	Removal rate	0.1	day^{-1}	[3]
$d(a)$	Probability at which an infected individual becomes severe	Figure S2	percent $\times 10^{-2}$	[4]
ω	Mortality rate of severe individuals	0.1	day^{-1}	Assumed
$\sigma(\tau)$	Vaccine efficacy in reducing the risk of infection	(2)	percent $\times 10^{-2}$	[9,10]
$\delta(\tau)$	Vaccine efficacy in reducing the risk of death	(2)	percent $\times 10^{-2}$	[9,10]
$h(a)$	Vaccine hesitancy rate	Figure S3	percent $\times 10^{-2}$	[5]
$\ell(a)$	Average life expectancy	Figure S8	Year	[11]
κ	Infection transmission rate	Determined according to $\mathcal{R}_0$	-	Assumed
$\beta_1(a)$	Age dependent susceptibility	Figure S6	-	Assumed
$\beta_2(x)$	Contact frequency among individuals whose age difference is x	Figure S6	-	Assumed
N	Total population in Japan	1.26×10^8	person	[6]
χ	Detection ratio	0.5	percent $\times 10^{-2}$	Assumed

Parameter setting

The unit time is set as 1 day. In Japan, the COVID-19 vaccination program for ordinary people started at April 12, 2021, and the booster (third) vaccination started at December 1, 2021. Because, in this study, we focus on the optimal interval between the first and second doses, we set the time range in our simulation from April 12, 2021 ($t = 0$) to November 30, 2021 ($t = t_{max} = 232$). As the vaccine age does not exceed the calendar time, we set $\tau_{max} = 232$. Let the unit age be 1 year, and the age interval be $[0,100]$, that is, $a_{max} = 100$.

We set $\varepsilon = 0.2$ and $\gamma = 0.1$ so that the average incubation period is $1/\varepsilon = 5$ days [1,2] and the average infectious period is $1/\gamma = 10$ days [3]. We assume that the severe class is composed of individuals who will die due to COVID-19, and set $d(a)$ as shown in Figure S2 by dividing the cumulative deaths by the cumulative cases in each age class as of November 30, 2021, using the open data in [4]. The vaccine hesitancy rate $h(a)$ is estimated as in Figure S3 using the vaccination data in [5].

For the initial condition, let

$$P_0(a) = S_0(a) + E_0(a) + I_0(a) + R_0(a) + W_0(a),$$

be the population age distribution in Japan as of April 2021 ($t = 0$). Using the data in [6], we fix $P_0(a)$ as shown in Figure S4. Here, we normalize $P_0(a)$ so that $\int_0^{a_{max}} P_0(a)da = 1$. Each population then describes a proportion to the total population. For simplicity, we assume that $W_0(a) = 0$, and fix $E_0(a), I_0(a)$ and $R_0(a)$ as shown in Figure S5 using the data in [4]. $S_0(a)$ can then be calculated as $P_0(a) - E_0(a) - I_0(a) - R_0(a)$.

We assume that the infection rate $\beta(a, b)$ has the following form:

$$\beta(a, b) = \kappa\beta_1(a)\beta_2(a - b),$$

where κ is the infection transmission rate, $\beta_1(a)$ is the age-dependent susceptibility, and $\beta_2(x)$ is a distance function representing the contact frequency among individuals whose age difference is x. More precisely, according to the three levels of heterogeneity (high, medium and low), we set $\beta_1(a)$ and $\beta_2(x)$ as follows (see Figure S6):

$$\beta_1(a) = \begin{cases} \text{Arctan}(-(a-65)/2)/\pi + 1/2, & \text{high,} \\ \text{Arctan}(-(a-65)/20)/\pi + 1/2, & \text{medium,} \\ \text{Arctan}(-(a-65)/80)/\pi + 1/2, & \text{low,} \end{cases}$$

$$\beta_2(x) = \begin{cases} f_{0,4}(x) + 0.15\left(f_{30,4}(x) + f_{-30,4}(x)\right) + 0.1\left(f_{60,4}(x) + f_{-60,4}(x)\right), & \text{high,} \\ f_{0,7}(x) + 0.5\left(f_{30,7}(x) + f_{-30,7}(x)\right) + 0.25\left(f_{60,7}(x) + f_{-60,7}(x)\right), & \text{medium,} \\ f_{0,10}(x) + 0.8\left(f_{30,10}(x) + f_{-30,10}(x)\right) + 0.6\left(f_{60,10}(x) + f_{-60,10}(x)\right), & \text{low,} \end{cases}$$

where $f_{\mu,\sigma}(x)$ denotes the probability density function of normal distribution with mean μ and standard derivation σ. $\beta_1(a)$ represents the heterogeneity in the age-dependent susceptibility (HS) and $\beta_2(x)$ represents the heterogeneity in the contact frequency among different age classes. The reason why we assume that $\beta_1(a)$ is higher in younger age group is that elderly people might be more careful and more likely to reduce the contact opportunity because the mortality of COVID-19 is

quite high in those people. The reason why we assume that $\beta_2(x)$ has five peaks is that the contact opportunity among children and their parents and grandparents might be high. In addition, we assume that if $\beta_2(x)$ (HC) is high, then people become more likely to contact with people in similar age group, whereas if $\beta_2(x)$ (HC) is low, then people become more likely to contact beyond age groups and the mixing becomes more homogeneous. The parameter κ is modified to fix the basic reproduction number $\mathcal{R}_0$ for different $\beta_1(a)$ and $\beta_2(x)$. Following the classical theory [7], $\mathcal{R}_0$ is defined by the spectral radius $r(K)$ of the following next generation operator K:

$$K\varphi(a) = \kappa P_0(a) \int_0^{a_{max}} \beta_1(a)\beta_2(a-b) \int_0^b e^{-\int_\rho^b [\gamma + d(\eta)]d\eta} \varphi(\rho)\, d\rho db.$$

We can numerically compute $r(K)$ by using a discretization method as in [8]. If we consider the case of $\mathcal{R}_0 = 1.5$, then κ is modified so that $r(K) = 1.5$ is attained (note that $r(K)$ is proportional to κ).

Let T be the length of the vaccination interval between the first and second doses. Assuming that severe individuals would not be newly vaccinated, the number of the first vaccination shots at time t is calculated as

$$\int_0^{a_{max}} v(t,a)[S(t,a) + E(t,a) + I(t,a) + R(t,a)]da \times N,$$

where $N = 1.26 \times 10^8$ is the total population in Japan as of 2021 [6]. The number of the second vaccination shots at time t is given by

$$\int_0^{a_{max}} [S_v(t,a,T) + E_v(t,a,T) + I_v(t,a,T) + R_v(t,a,T)]da \times N.$$

We assume that the vaccination rate is separable:

$$(1)\quad v(t,a) = v_1(t)v_2(a).$$

It then follows that

$$v_1(t) = \frac{V(t)/N - \int_0^{a_{max}} [S_v(t,a,T) + E_v(t,a,T) + I_v(t,a,T) + R_v(t,a,T)]da}{\int_0^{a_{max}} v_2(a)[S(t,a) + E(t,a) + I(t,a) + R(t,a)]da},$$

where $V(t)$ denotes the total number of vaccination at time t. We fix $V(t)$ as shown in Figure S7 using the data of vaccine distribution for COVID-19 in Japan from April 12, 2021 to November 30, 2021 [5]. $v_2(a)$ can be used to incorporate the priority of vaccine allocation to individuals aged a. We assume that

$$v_2(a) = \begin{cases} 0, & 0 \le a < 18, \\ 1-u, & 18 \le a < 65, \\ u, & a \ge 65, \end{cases}$$

where $u \in [0.1, 0.9]$ denotes the ratio of vaccine allocation to those aged over 65. The vaccine efficacy is set as

$$(2)\quad \sigma(\tau)=\begin{cases}0, & 0\le\tau<14,\\ \sigma_1[1-k(\tau-14)], & 14\le\tau<T,\\ \sigma_2[1-k(\tau-T)], & \tau\ge T,\end{cases}\qquad \delta(\tau)=\begin{cases}0, & 0\le\tau<14,\\ \delta_1[1-k(\tau-14)], & 14\le\tau<T,\\ \delta_2[1-k(\tau-T)], & \tau\ge T,\end{cases}$$

where σ_i and δ_i $(i=1,2)$ denote the efficacy of the i-th vaccination in reducing the risk of infection and the risk of disease-related death, respectively. Here, according to [9], we assume that the vaccine efficacy linearly decreases with waning rate $k>0$. In this study, we fix $k=1/600$ so that the efficacy decreases to its half after 300 days passed [9]. We consider the Pfizer and AstraZeneca vaccines taking the mean of a dataset in [10]:

$$(\sigma_1,\sigma_2,\delta_1,\delta_2)=\begin{cases}(0.63,0.90,0.80,0.94), & \text{Pfizer},\\ (0.62,0.64,0.80,0.85), & \text{AstraZeneca}.\end{cases}$$

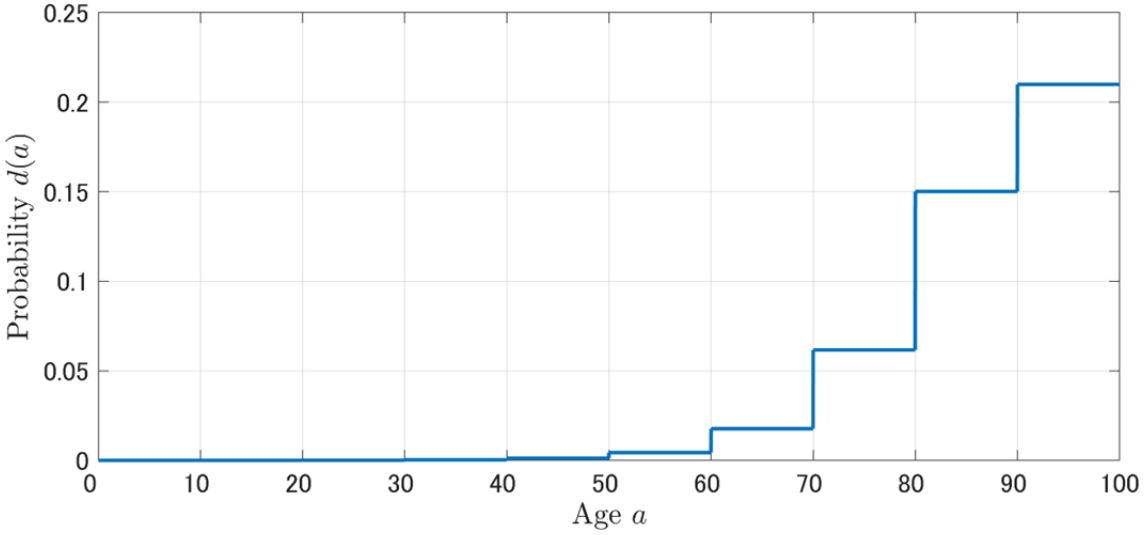

Figure S2. Age-specific probability at which a recovered individual becomes severe.

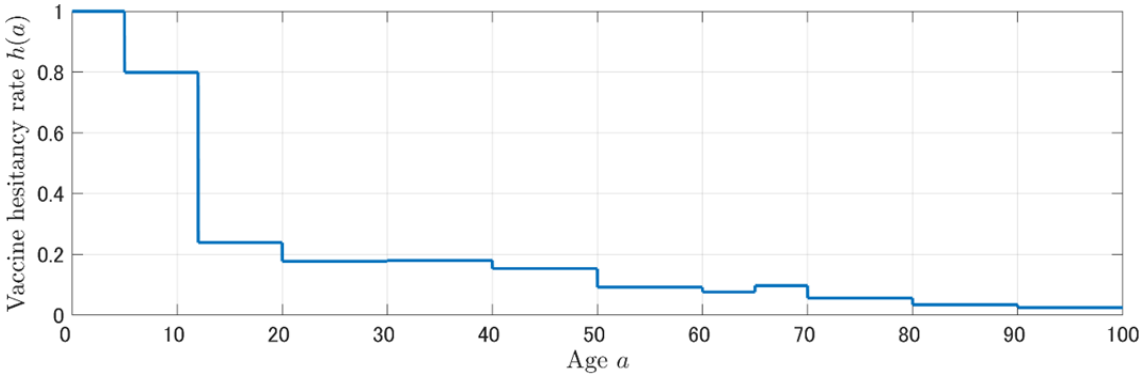

Figure S3. Age-specific vaccine hesitancy rate h(a).

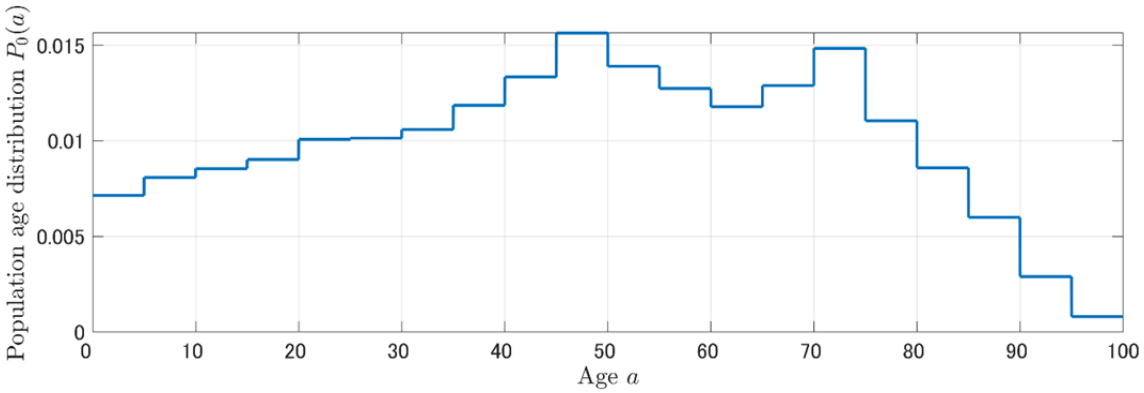

Figure S4. Initial population age distribution $P_0(a)$.

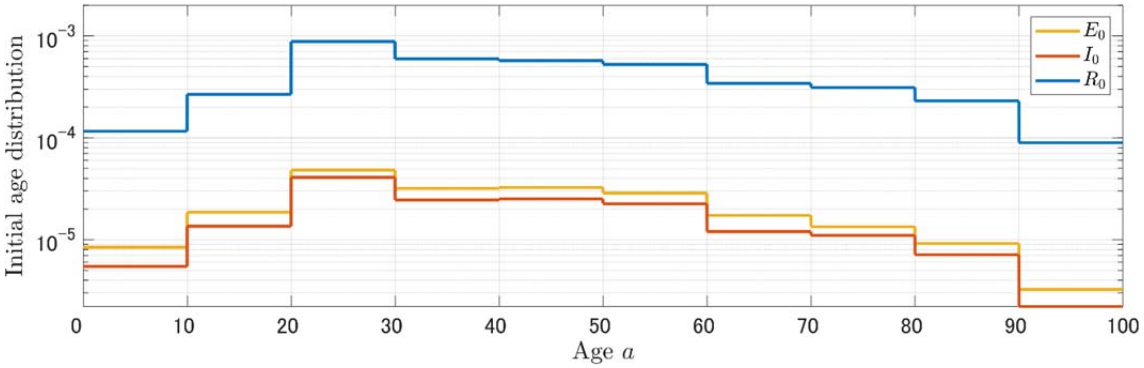

Figure S5. Initial age distributions of exposed $E_0(a)$, infectious $I_0(a)$ and recovered $R_0(a)$ populations.

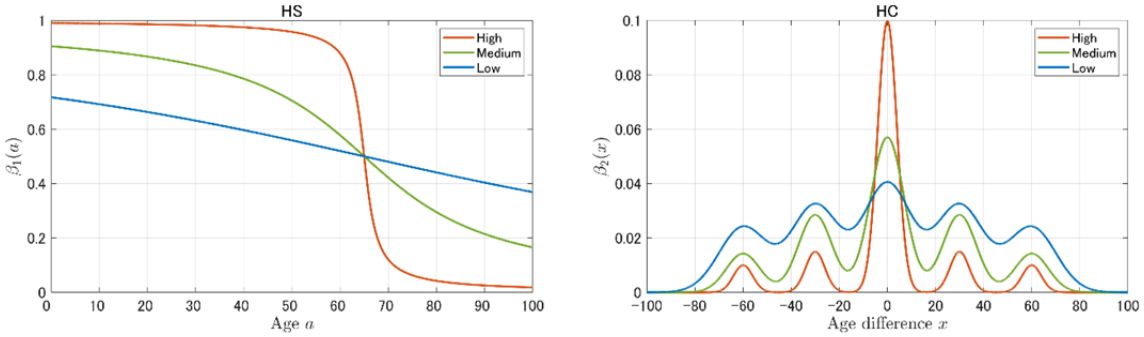

Figure S6. Age dependent susceptibility $\beta_1(a)$ (HS) and contact frequency $\beta_2(x)$ among individuals whose age difference is x (HC). Three levels of heterogeneity (high, medium and low) are considered to each of them.

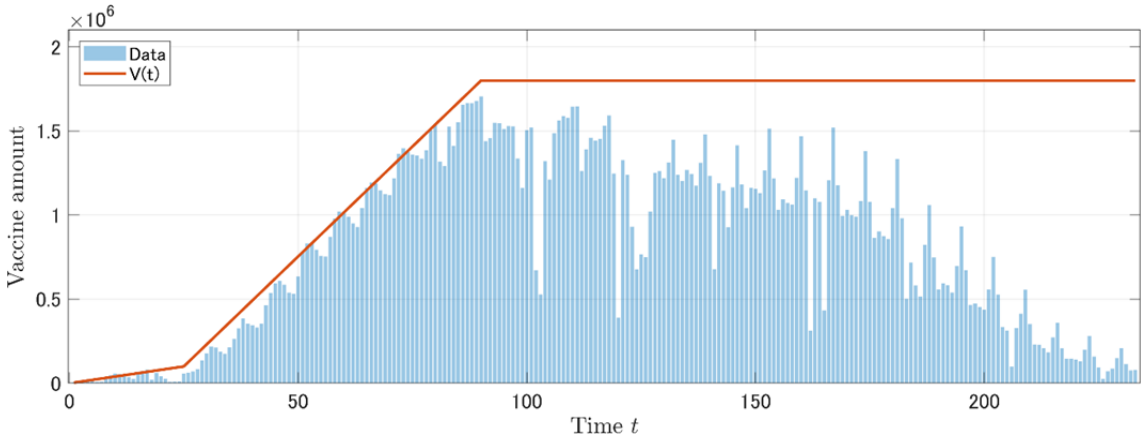

Figure S7. Daily number of vaccination shots in Japan from April 12, 2021 to November 30, 2021.

Objective functions

To evaluate the effectiveness of vaccination program, we calculate the total number of cases as

$$H_1 = \int_0^{t_{max}} \int_0^{a_{max}} \lambda(t,a)\left\{S(t,a) + S_h(t,a) + \int_0^{\tau_{max}} [1-\sigma(\tau)]S_v(t,a,\tau)d\tau\right\} da\, dt \times N,$$

and the total number of disease-induced deaths as

$$H_2 = \omega \int_0^{t_{max}} \int_0^{a_{max}} [W(t,a) + W_h(t,a) + W_v(t,a)] da\, dt \times N.$$

Let $\ell(a)$ be the average life expectancy at age a, which is estimated from the data in [11] as shown in Figure S8. The total number of disease-induced deaths weighted by the average life expectancy is as follows:

$$H_3 = \omega \int_0^{t_{max}} \int_0^{a_{max}} \ell(a)[W(t,a) + W_h(t,a) + W_v(t,a)] da\, dt \times N.$$

To compute the reduction ratio, we divide each of these functions by those without vaccination ($V(t) = 0$).

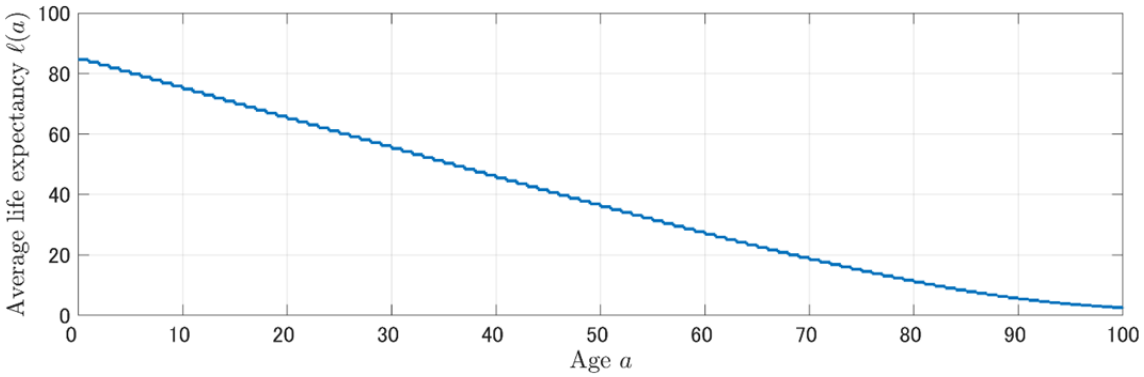

Figure S8. Age-specific average life expectancy $\ell(a)$.

Counterfactual simulation for Japan in 2021

For the baseline scenario, we assume that the vaccination interval between the first and second doses is 3 weeks, the vaccine efficacy is as of Pfizer, the ratio u of vaccine allocation to the elderly people is 0.9, and both β_1 and β_2 are medium. We then estimate the time-varying infection rate with $\kappa = \kappa(t)$ by fitting the following function to the daily reported cases in Japan:

$$Y(t) := \chi \int_0^{a_{max}} \lambda(t,a) \left\{ S(t,a) + S_h(t,a) + \int_0^{\tau_{max}} [1-\sigma(\tau)] S_v(t,a,\tau) d\tau \right\} da \times N,$$

where χ is the detection ratio, that is, the ratio at which a newly infected individual is finally reported. More precisely, to estimate the infection rate on a day, we compare the simulation result and the real data of the newly reported cases in past 7 days, and find the parameter that minimizes the sum of the squares error. In our simulation, we assume that $\chi = 0.5$. The comparison of the curve of $Y(t)$ and the real data [4] is shown in Figure S9, top. Note that this function $Y(t)$ is uniquely calculated. For this estimated infection rate, we compare the daily number of newly reported deaths

$$D(t) = \omega \int_0^{a_{max}} [W(t,a) + W_h(t,a) + W_v(t,a)] da \times N,$$

and the real data [4] as shown in Figure S9, bottom. Here, for a technical reason on the fitting of $D(t)$, we compare the total deaths in the period from May 15, 2021 to November 30, 2021. Regarding this setting as a baseline, we investigate how the total deaths could be reduced if the optimal vaccination interval and the optimal ratio of allocation to the elderly people had been taken.

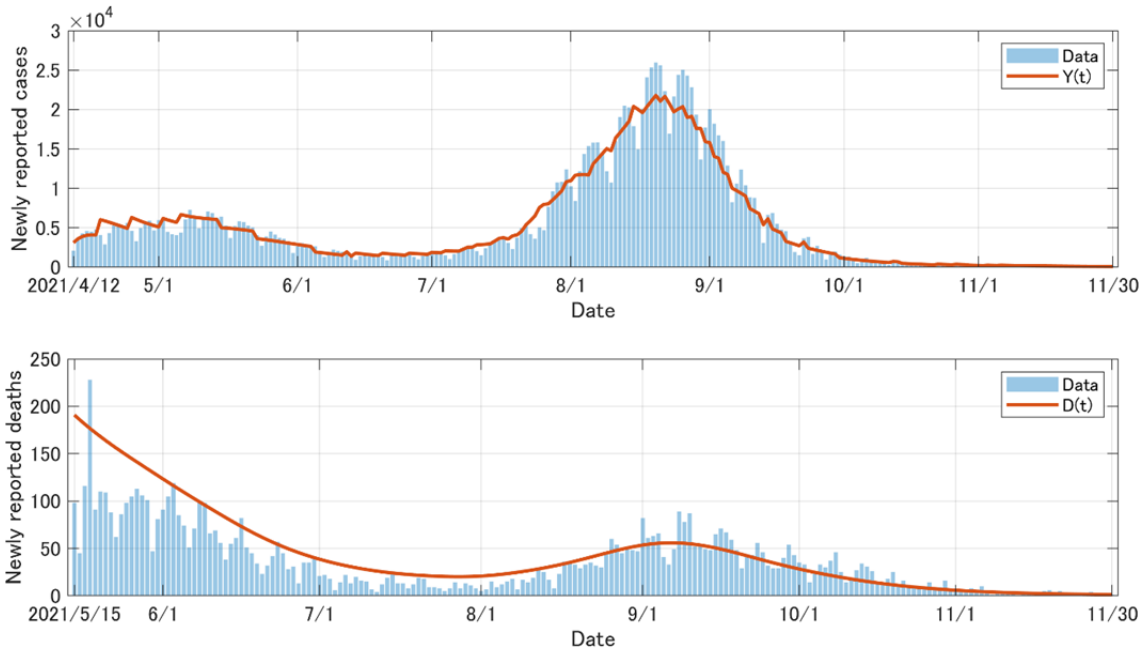

Figure S9. Daily number of newly reported cases (top) and deaths (bottom). Functions $Y(t)$ and $D(t)$ are derived from our model.

Numerical scheme

To run the simulation program, we use the standard Euler forward method. See Figure S10 for the main part of the program code for MATLAB.

```
for t=1:1:nt-1
    for a=1:1:na
        f1(a)=Sv(t,a,T)+Ev(t,a,T)+Iv(t,a,T)+Rv(t,a,T);
        f2(a)=v2(a)*(S(t,a)+E(t,a)+I(t,a)+R(t,a));
    end
    F1=sum(f1)*da;
    F2=sum(f2)*da;
    v1(t)=max((V(t)/N-F1)/F2,0);

    for a=1:1:na
        v=v1(t)*v2(a);

        for b=1:1:na
            bI(a,b)=bet(a,b)*(I(t,b)+Ih(t,b)+sum(Iv(t,b,1:1:nx))*dx);
        end
        lam=sum(bI(a,:))*da;

        S(t+1,a)=S(t,a)+dt*(-lam*S(t,a)-v*S(t,a));
        E(t+1,a)=E(t,a)+dt*(lam*S(t,a)-eps*E(t,a)-v*E(t,a));
        I(t+1,a)=I(t,a)+dt*(eps*E(t,a)-gam*I(t,a)-v*I(t,a));
        R(t+1,a)=R(t,a)+dt*((1-d(a*da))*gam*I(t,a)-v*R(t,a));
        W(t+1,a)=W(t,a)+dt*(d(a*da)*gam*I(t,a)-om*W(t,a));

        Sh(t+1,a)=Sh(t,a)+dt*(-lam*Sh(t,a));
        Eh(t+1,a)=Eh(t,a)+dt*(lam*Sh(t,a)-eps*Eh(t,a));
        Ih(t+1,a)=Ih(t,a)+dt*(eps*Eh(t,a)-gam*Ih(t,a));
        Rh(t+1,a)=Rh(t,a)+dt*((1-d(a*da))*gam*Ih(t,a));
        Wh(t+1,a)=Wh(t,a)+dt*(d(a*da)*gam*Ih(t,a)-om*Wh(t,a));

        Sv(t+1,a,1)=v*S(t,a);
        Ev(t+1,a,1)=v*E(t,a);
        Iv(t+1,a,1)=v*I(t,a);
        Rv(t+1,a,1)=v*R(t,a);

        SS(1)=(1-Sig(1))*lam*Sv(t,a,1);
        for x=2:1:nx
            Sv(t+1,a,x)=Sv(t,a,x)+dt*(-(Sv(t,a,x)-Sv(t,a,x-1))/dx...
                -(1-Sig(x))*lam*Sv(t,a,x-1));
            Ev(t+1,a,x)=Ev(t,a,x)+dt*(-(Ev(t,a,x)-Ev(t,a,x-1))/dx...
                +(1-Sig(x))*lam*Sv(t,a,x-1)-eps*Ev(t,a,x-1));
            Iv(t+1,a,x)=Iv(t,a,x)+dt*(-(Iv(t,a,x)-Iv(t,a,x-1))/dx...
                +eps*Ev(t,a,x-1)-gam*Iv(t,a,x-1));
            Rv(t+1,a,x)=Rv(t,a,x)+dt*(-(Rv(t,a,x)-Rv(t,a,x-1))/dx...
                +(1-(1-Del(x))*d(a))*gam*Iv(t,a,x-1));
            WW(x)=(1-Del(x))*d(a)*gam*Iv(t,a,x-1);
            SS(x)=(1-Sig(x))*lam*Sv(t,a,x);
        end
    end
end
```

Figure S10. The main part of our simulation code for MATLAB. Some symbols are defined in other parts or files.

References

1. S. A. Lauer, K. H. Grantz, Q. Bi, F. K. Jones, Q. Zheng, H. R. Meredith, et al, The incubation period of coronavirus disease 2019 (COVID-19) from publicly reported confirmed cases: estimation and application, *Ann. Intern. Med.*, **172** (2020), 577–582. https://doi.org/10.7326/M20-0504
2. N. M. Linton, T. Kobayashi, Y. Yang, K. Hayashi, A. R. Akhmetzhanov, S. Jung, et al., Incubation period and other epidemiological characteristics of 2019 novel coronavirus infections with right truncation: A statistical analysis of publicly available case data, *J. Clin. Med.*, **9** (2020), 538. https://doi.org/10.3390/jcm9020538
3. A. W. Byrne, D. McEvoy, A. B. Collins, K. Hunt, M. Casey, A. Barber, et al., Inferred duration of infectious period of SARS-CoV-2: rapid scoping review and analysis of available evidence for asymptomatic and symptomatic COVID-19 cases, *BMJ Open*, **10** (2020), e039856. https://doi.org/10.1136/bmjopen-2020-039856
4. *Ministry of Health, Labour and Welfare of Japan*, Visualizing the data: information on COVID-19 infections. Available from: https://covid19.mhlw.go.jp/en/
5. *Digital Agency*, Vaccination Record System (VRS). Available from: https://info.vrs.digital.go.jp/opendata/ (Japanese)
6. *Statistics of Japan*, Re-calculated on the complete counts of the 2020 Population Census (Oct. 2020 – June 2021). Available from: https://www.stat.go.jp/english/data/jinsui/2.html
7. O. Diekmann, J. A. P. Heesterbeek, J. A. J. Metz, On the definition and the computation of the basic reproduction ratio R0 in models for infectious diseases in heterogeneous populations, *J. Math. Biol.*, **28** (1990), 365–382. https://doi.org/10.1007/BF00178324
8. T. Kuniya, Numerical approximation of the basic reproduction number for a class of age-structured epidemic models, *Appl. Math. Lett.*, **73** (2017), 106–112. http://dx.doi.org/10.1016/j.aml.2017.04.031
9. S. Kodera, E. A. Rashed, A. Hirata, Estimation of real-world vaccination effectiveness of mRNA COVID-19 vaccines against delta and omicron variants in Japan, *Vaccines*, **10** (2022), 430. https://doi.org/10.3390/vaccines10030430
10. *SPI-M-O*, Summary of further modelling of easing restrictions – Roadmap Step 2 (2021). Available from: https://assets.publishing.service.gov.uk/government/uploads/system/uploads/attachment_data/file/975909/S1182_SPI-M-O_Summary_of_modelling_of_easing_roadmap_step_2_restrictions.pdf
11. *Ministry of Health, Labour and Welfare of Japan*, Life Tables. Available from: https://www.mhlw.go.jp/english/database/db-hw/vs02.html.

AIMS Press